JOURNAL OF APPLIED POLYMER SCIENCE VOL. 15, PP. 183-197 (1971)

Necking of High-Density Polyethylene

YASAKU WADA, *Department of Applied Physics, Faculty of Engineering, University of Tokyo, Bunkyo-ku, Tokyo, Japan,* and AKIRA NAKAYAMA, *Department of Fiber Engineering, Faculty of Engineering, Gifu University, Kagamihara City, Gifu Prefecture, Japan*

Synopsis

Necking draw of high-density polyethylene is studied at draw rates of 2.5×10^{-2} to 25 mm/min and at temperatures of $-40°$ to 80°C. Effect of temperature and draw rate on necking stress is interpreted in terms of viscoelastic flow of amorphous phase accompanying orientation of crystallites. It is proved that reducibility of draw rate and temperature holds and that the reduction factor obeys approximately the Williams-Landel-Ferry equation. Necking stress at an extremely low draw rate, critical necking stress, is discussed in terms of the phase equilibrium under stress between two states before and after microfracture of crystallites. The theory, with some approximations, leads to the equation by Iida in which the critical necking stress is expressed by fusion parameters. The thermodynamic behavior of isothermal necking is discussed and a phenomenologic criterion for necking is presented.

INTRODUCTION

Most polymers under the proper conditions will cold draw. In the first region of stress–strain relation, the curve is almost linear and the specimen stretches uniformly. At the yield point, the neck forms in one region of the specimen and the stress reaches a maximum (yield stress) and then drops to a slightly smaller value at which it remains constant (necking stress) as the stretching continues. In this second region there exist undrawn and drawn regions in the specimen. The drawn region grows at the expense of the undrawn region till the neck reaches the end.

Cold drawing with necking occurs with amorphous polymers at temperatures somewhat below the glass temperature.[1–6] With crystalline polymers, the cold drawing takes place from the glass temperature up to near the melting point.[5–8] Some polymers yield homogeneously rather than form the neck at very small draw rates, but high-density polyethylene forms a neck even at extremely slow draw rates.[8]

Change in crystalline structure of polyethylene with cold drawing was extensively studied by Kasai and Kakudo[9] by use of x-ray wide-angle diffraction and small-angle scattering. According to them, the structure changes rapidly in the neck zone from the initial unoriented crystallites to perfectly *c*-axis-oriented crystallites.

A thermodynamic theory of necking that takes into account the equilib-

rium among these phases was first proposed by Müller and Jäckel[10–13] and recently by Iida,[14] who interpreted the necking stress at an extremely low draw rate (critical necking stress) in terms of fusion parameters. A rheological theory of necking was also developed by several authors[2,6,12] with the purpose of interpreting the draw rate dependence of necking stress.

In the present paper, experimental results of necking of high-density polyethylene, especially at low temperatures and at low draw rates, will be presented. A four-state model for necking is proposed on the basis of observation by Kasai and Kakudo,[9] and the behavior of necking is theoretically analyzed. Dependence of necking stress on temperature and draw rate is interpreted in terms of viscoelasticity of amorphous region and orientation rate of crystallites. Temperature dependence of critical necking stress is thermodynamically discussed. Finally, a phenomenologic criterion for necking will be suggested.

EXPERIMENTAL

The necking phenomena of high-density polyethylene were studied in detail by Iida[14] above room temperature and at draw rates higher than 1 mm/min by use of a conventional tensile tester. For the purpose of extending the ranges of temperature and draw rate, a device for measuring stress–strain curves was designed, as illustrated in Figure 1.

The lower end of the specimen was clamped in the liquid bath, and the upper end was drawn upward at a constant speed by means of a synchronous motor with reduction gear boxes. The draw rate ranged from 2.5×10^{-2} to 25 mm/min. The tensile force was measured by a phosphorus-bronze ring to which four wire resistance strain gauges were cemented. The gauges were connected to make a Wheatstone bridge for the purpose of eliminating temperature effect. The output from the bridge, which is proportional to the tensile force, was recorded as a function of time by an automatic balancing dc potentiometer.

The temperature of the specimen was controlled by a liquid bath with water and methanol–Dry Ice mixture above and below room temperature,

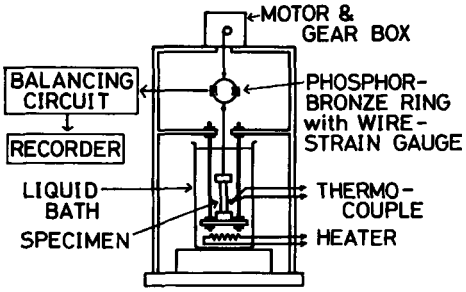

Fig. 1. Apparatus for measuring stress–strain relation at constant elongation rate.

respectively. The temperature was measured by a Cu-Constantan thermocouple.

Specimens were cut out from the 0.04-mm-thick vacuum-pressed film (Marlex 6002). The film was proved to be isotropic from elasticity measurement. The specimen was 5 mm in width and the span length was 15 mm. The specimen was marked by ink in order to measure the draw ratio after necking.

Three pieces of specimens were used for a single temperature and draw rate, and necking stress σ_N was expressed by the tensile force per unit cross-sectional area of initial state (conventional stress); yield strain s_N at which necking starts and draw ratio α_N (ratio in length of drawn region to initial one) were obtained as average.

Density of specimen before and after draw was measured by a density gradient tube of benzene–CCl_4 mixtures. The density before draw was 0.967 g/cm^3 (30°C) and after draw, at 80°C and a draw rate 25 mm/min, for example, 0.967, 0.966, and 0.965 g/cm^3 (30°C) for undrawn region, neck region, and drawn region, respectively. The results, together with those under other draw conditions, indicate that the density variation in the course of necking is relatively small.

Use of thin specimens in a liquid bath in the present study makes it possible to assume that the process is almost isothermal and that temperature rise in the specimen by drawing is relatively insignificant.

RESULTS

Four-State Model for Necking of Polyethylene

A three-state model has been proposed by Iida[14] for interpreting neck draw of high-density polyethylene: randomly oriented crystals, oriented melt, and *c*-axis-oriented crystals. For understanding draw rate dependence of necking stress, however, a four-state model seems to be more convenient, as will be described in the following.

According to Kasai and Kakudo,[9] the undrawn region of polyethylene, designated phase A in the following, has an unoriented spherulitic structure. In the early stage of the neck region, which will be denoted phase B_1, the *a*-axis of crystallites is preferentially oriented perpendicularly to the draw direction, but the orientation of the *b*- and *c*-axis is rather random. The spherulite deforms to an ellipsoid, with the major axis parallel to the draw direction. In the later stage of the neck region, phase B_2, the *c*-axis is preferentially oriented along the draw direction. Finally in the drawn region, phase C, the *c*-axis is almost completely oriented along the draw direction, and the polymer has a fibrous structure. In the course of B_1 to B_2, each crystallite is deformed and fractured into small blocks, and new crystallites are formed in phase C.[15]

Of course, such a change in structure takes place continuously during neck draw, but the four-state model in Figure 2 may be convenient for understanding the necking phenomena. In this study, the necking be-

A (unoriented crystallites)
↓ ← orientation of crystallites accompanied with viscoelastic flow of amorphous phase.
B_1 (moderately oriented crystallites before microfracture)
↓ ← microfracture of crystallites, separation of crystallite into blocks.
B_2 (oriented phase with numerous defects)
↓ ← gathering of blocks
C (*c*-axis-oriented crystallites of fiber structure)

Fig. 2. Four-state model for necking of polyethylene.

havior of high-density polyethylene will be interpreted in terms of the four-state model.

Necking Stress as a Function of Draw Rate and Temperature

Figure 3 illustrates the necking stress σ_N as a function of draw rate R. The data by Iida[14] for annealed high-density polyethylene (Sholex 6009) are in good agreement with ours in the overlapping range of draw rate and temperature and were used, together with those of the present work, in the following analysis.

Cold draw with necking in high-density polyethylene does not occur below −50°C, which is just the lower limit of glass transition region of this polymer.[16] Above this temperature, the necking stress depends markedly on both draw rate and temperature. The dependence may be interpreted in terms of viscoelasticity of amorphous phase among crystallites.

Since the most time-dependent and temperature-dependent process in the four-state model in Figure 2 is the reaction A → B_1, we assume, except at

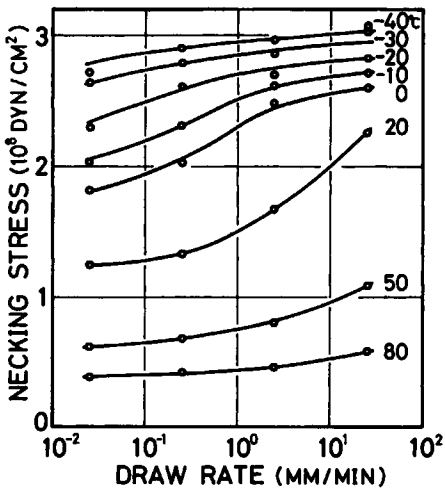

Fig. 3. Necking stress of high-density polyethylene plotted against draw rate for various temperatures.

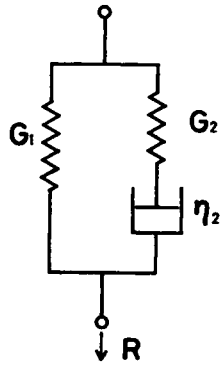

Fig. 4. Three-element model of a highly crystalline polymer.

extremely low draw rates, that this reaction is the rate-determining process of necking. As is well known, high-density polyethylene has a spherulitic structure, and each spherulite contains numerous lamellae and 10–20% of amorphous phase. The following considerations are, however, based on a simple model in which, as far as the reaction A → B_1 is concerned, each crystallite is assumed to be oriented as a rigid body under uniaxial stress in the matrix of the amorphous phase.

If the specimen is sufficiently slowly drawn compared with the viscoelastic relaxation time of the amorphous phase, the crystallite will be well oriented so that the succeeding process $B_1 \rightarrow B_2$, the microfracture of crystals by generation and slip of dislocations in the crystal, can easily occur and hence σ_N may be low. On the contrary, if the specimen is drawn too rapidly, the crystallite has no time to be oriented so that only a minor component of applied stress may be effective in the process $B_1 \rightarrow B_2$, and hence σ_N may be high. Since the relaxation time τ of the amorphous phase decreases with increasing temperature, σ_N at a specified value of R decreases with increase in temperature. Such an interpretation is quite parallel to that by Nakada and co-workers[17] for temperature and draw rate dependence of yield stress.

A model of crystalline polymers is given in Figure 4, where a spring G_1 represents crystallites and a series connection of spring G_2 and dashpot η_2 represents the amorphous region. The deformation of G_1 does not mean the deformation of crystallites, but orientation. The model is based on the fact that the orientation of crystallites with draw must be accompanied by viscoelastic flow of the amorphous region.

When the model in Figure 4 is drawn with a constant rate R, the stress in G_1 is

$$\sigma_1 = G_1 s \tag{1}$$

where s is the strain. The stress in G_2 and η_2 is

$$\sigma_2 = G_2 R\tau[1 - \exp(-s/R\tau)] \tag{2}$$

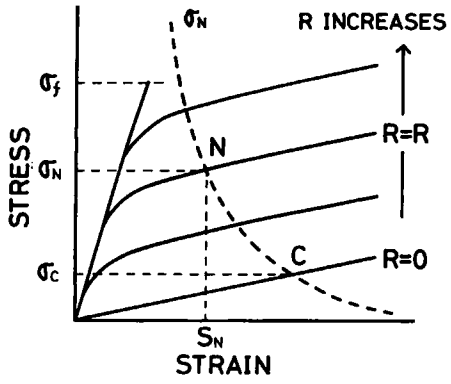

Fig. 5. Schematic representation of stress–strain relations of the model in Fig. 4 for various draw rates R (solid curves). Dashed curve represents necking stress σ_N as a function of yield strain s_N; σ_f represents stress for brittle fracture.

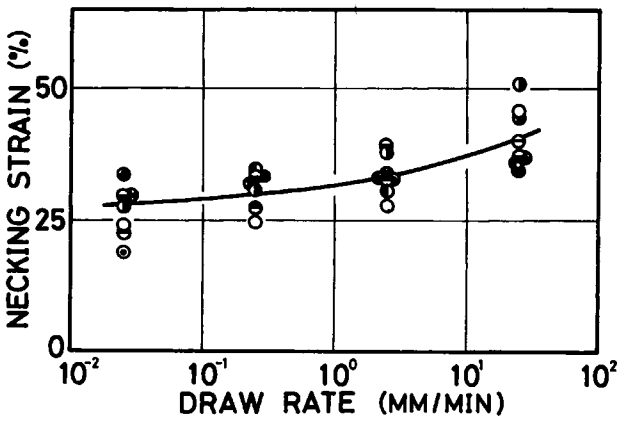

Fig. 6. Necking strain (or yield strain at which necking starts) of high-density polyethylene plotted against draw rate for various temperatures: (○) 80°C; (◑) 50°C; (◒) 20°C; (⊙) 0°C; (◐) −10°C; (●) −20°C; (⊗) −30°C; (◓) −40°C.

where τ is the relaxation time and is defined by $\tau = \eta_2/G_2$. Then the total stress σ is

$$\sigma = \sigma_1 + \sigma_2 = G_1 s + G_2 R\tau[1 - \exp(-s/R\tau)]. \quad (3)$$

At a small value of s, σ is approximated by $(G_1 + G_2)s$, and at a large value of s, σ approaches $(G_1 s + \eta_2 R)$. In Figure 5, σ is schematically shown as a function of s by solid lines for various values of R.

As has been described, the necking stress will decrease with increasing crystallite orientation, that is, with increasing s. The curve σ_N versus s is drawn in Figure 5 by a dashed line. The intersecting point with the solid line gives σ_N and s_N as a function of R. The σ_N value decreases with decreasing R and finally reaches σ_c at $R = 0$, which may be called, according to Iida,[14] the critical necking stress. The solid line has, therefore, a

physical significance only below σ_N because, when neck starts at s_N, σ is kept constant at σ_N.

When R is extremely high, the σ verus s curve reaches a critical value σ_f (brittle fracture stress) before meeting the σ_N curve. This indicates that the specimen undergoes brittle fracture when the draw rate is too high.

The relation between σ_N and s_N is given from eq. (3) as

$$\sigma_N = G_1 s_N + G_2 R\tau[1 - \exp(-s_N/R\tau)]. \quad (4)$$

Experimental results for s_N, strain at which neck starts or yield occurs, are drawn in Figure 6 as a function of draw rate. As readily seen, the dependence of s_N on draw rate and temperature is not so significant. According to Nakada,[17] who measured s_N up to an extremely high draw rate (10^{4}%/min), s_N decreases relatively gradually with increasing draw rate. These results indicate that s_N does not vary so much with R and temperature within the range of the present study, and σ_N is expected to be a function of $R\tau$ from eq. (4).

Since the instantaneous elastic modulus G_2 is nearly independent of temperature and the contribution of $G_1 s$ to σ_N is small, temperature dependence of σ_N is largely determined by that of τ. Under these assumptions, we can conclude the reducibility of draw rate and temperature, in a similar way to the well-known time–temperature reducibility in viscoelasticity of amorphous polymers.[18]

Temperature dependence of τ is written as

$$\tau(T) = a_T \tau(T_0) \quad (5)$$

where T_0 is an arbitrary reference temperature and a_T is a function of temperature T (shift factor). Then it follows from eq. (4) that

$$\sigma_N(R, T) = \sigma_N(a_T R, T_0). \quad (6)$$

Equation (6) indicates that the curve $\sigma_N(T)$ plotted against log R may be superposed on curve $\sigma_N(T_0)$ by shifting along the horizontal axis. The shift value is equal to log a_T.

In Figure 7, the master curve is obtained by the above procedure from the data in Figure 3 and the data by Iida.[14] The curves of σ_N against log R at various temperatures are well superposed into a single curve.

Figure 8 illustrates the shift factor log a_T plotted against temperature, giving the temperature dependence of relaxation time. The activation energy H was calculated by the equation

$$H = (\log_e 10) R \frac{\partial \log a_T}{\partial(1/T)}. \quad (7)$$

A value for H of 40 kcal/mole was obtained around 50°C, which is reasonable as the activation energy of viscosity of amorphous phase above glass transition temperature. The plot of log a_T in Figure 8 might be fitted by the Williams-Landel-Ferry equation,[19] but the values at low temperatures

are slightly lower than expected from the equation. It must be noted that the applicability of the superposition principle in the present case is based on the simple model with some approximations. Exact treatment should include the distribution of relaxation times and nonlinearity for the

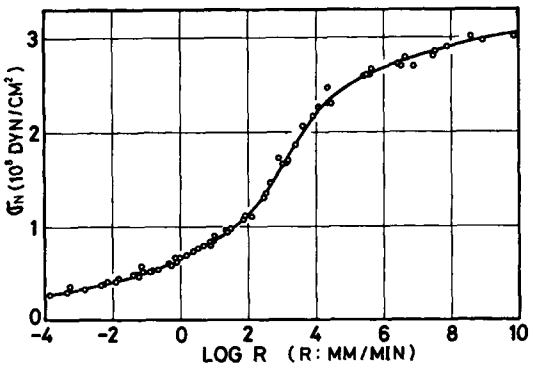

Fig. 7. Master curve of necking stress of high-density polyethylene plotted against draw rate obtained by horizontal shift of curves in Fig. 3 and those by Iida.[14] Reference temperature 60°C.

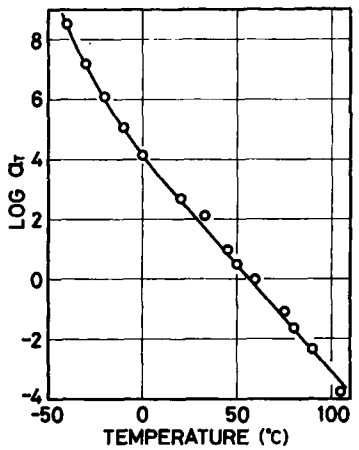

Fig. 8. Shift factor of necking stress of high-density polyethylene as a function of temperature. Reference temperature 60°C.

viscoelasticity of the amorphous phase. The necking stress at $R = 0$, which was assumed constant in the horizontal shift, varies with temperature, as will be fully discussed in the next section.

Necking viscosity η_N, which is defined by $\eta_N = \sigma_N/R$, is given from eq. (4) to be

$$\eta_N = \frac{G_1 s_N}{R} + G_2\tau[1 - \exp(-s_N/R\tau)]. \tag{8}$$

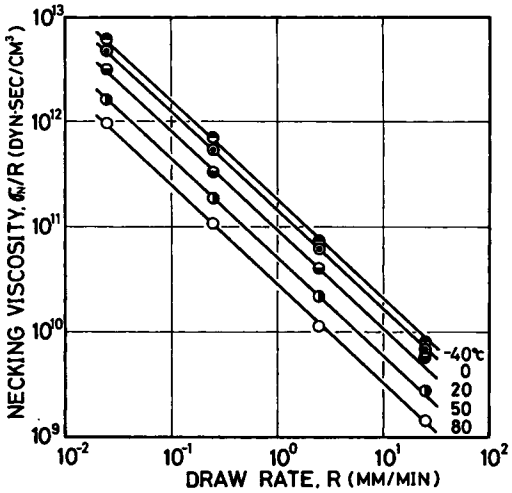

Fig. 9. Necking viscosity of high-density polyethylene plotted against draw rate for various temperatures.

η_N decreases with increasing R; and for $R\tau > s_N$, η_N is expanded in the series

$$\eta_N = \frac{(G_1+G_2)s_N}{R} - \frac{G_2 s_N^2}{2R^2\tau} + \cdots\cdots \tag{9}$$

The result in Figure 9, where log η_N is plotted against log R for various temperatures, indicates that η_N is proportional to $R^{-0.93}$. According to Iida,[14] who measured η_N of high-density polyethylene in a relatively high range of R (R = 1 to 10^6 mm/min), η_N is proportional to $R^{-0.75}$ for various temperatures (33° to 105°C). These results indicate that η_N is proportional to R^{-n}, where n is slightly smaller than unity, which is quite reasonable from eq. (9), taking into account that s_N is almost independent of R for small R but slightly decreases for large R values.[17]

It should be emphasized that the draw rate dependences of necking stress and necking viscosity are interpreted here in terms of linear viscoelasticity of the amorphous phase. More exact treatment will require, however, to take into account the nonlinearity of this parameter.

Critical Necking Stress

As has been described in the preceding section, the necking stress at a low enough draw rate will approach a constant value, σ_c. The curves in Figure 3 seem to level off at a constant value when extrapolated to $R \to 0$.

The value of the critical necking stress σ_c is given as $G_1 s_N$ by the model in Figure 4, but the physical meaning of this expression is rather obscure because the model is taken only for the interpretation of the rheological behavior of σ_N. In discussing σ_c, therefore, we consider the phase equilibrium in the four-state model in Figure 2. The first step $A \to B_1$, which is

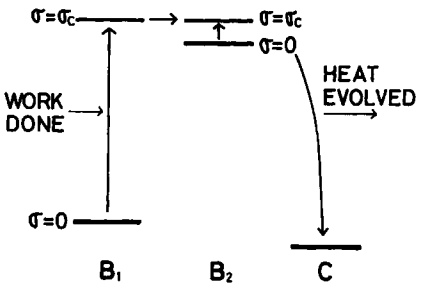

Fig. 10. Schematic representation of free energy levels of the three states without and with applied stress.

significant at a finite draw rate, may be always in equilibrium at an extremely low draw rate, and the succeeding reactions $B_1 \rightarrow B_2 \rightarrow C$ must be considered.

Figure 10 illustrates the energy per unit volume of states B_1, B_2, and C. Since the states B_1 and C correspond to two crystalline phases, respectively, which are different in orientation but similar in crystallinity, the two states may have a similar energy level at zero stress. The state B_2, on the other hand, includes a large amount of defects and hence may have a higher energy. The defects in B_2 are bound by an energy barrier, and consequently this phase actually exists as a metastable phase.

When the stress is applied, the energy level is elevated by a different amount for the three states. Since crystallites in state C are completely oriented, the stress cannot change the energy any more. On the other hand, the energy of state B_1, in which crystallites are only moderately oriented, will be appreciably increased by stress. In other words, external stress can do much work in state B_1 but none in state C. The energy variation of the three states with stress is shown in Figure 10. When the stress reaches a critical value σ_c, the energy levels of B_1 and B_2 become equal; and, if this energy is high enough for defects in B_2 to move, the reaction $A \rightarrow B_1 \rightarrow B_2 \rightarrow C$ proceeds irreversibly. The work done by the stress in the process of $A \rightarrow B_1 \rightarrow B_2$ is irreversibly dissipated as heat in the process of $B_2 \rightarrow C$. If the internal energy is the same in the initial and final states, A and C, heat equal to work done by the stress will be evolved in the course of necking.

The condition of determining σ_c is therefore

$$u_1(\sigma_c) = u_2(\sigma_c) \tag{10}$$

where u_1 and u_2 are the Gibb's free energy per unit volume of states B_1 and B_2, respectively. We assume $u(\sigma)$ can be expressed as

$$u(\sigma) = H - TS + \sigma(\alpha_c - \alpha) \tag{11}$$

where H and S are the enthalpy and entropy at zero stress, α is the local draw ratio, and α_c is the upper limit of α. The term $\sigma(\alpha_c - \alpha)$ represents

the increase of free energy by the stress. Since the state B_1 has a smaller value of α than B_2, the increase of free energy by the stress is larger.

Equations (10) and (11) lead to

$$\sigma_c = \frac{\Delta H - T\Delta S}{\Delta\alpha} \tag{12}$$

where ΔH, ΔS, and $\Delta\alpha$ are differences in enthalpy, entropy, and draw ratio, respectively, between the states B_2 and B_1 at zero stress.

If the state B_2 is approximated by liquid or melt, ΔH and ΔS mean the enthalpy and entropy of fusion multiplied by the degree of crystallinity, $X_c\Delta H_m$ and $X_c\Delta S_m$, respectively. Furthermore, if the draw ratio α is assumed equal in A and B_1 and in B_2 and C, $\Delta\alpha$ corresponds to the difference in α between C and A, which is equal to $(\alpha_N - 1)$ and can be measured from the necking draw ratio α_N. Then we obtain the equation

$$\sigma_c = \frac{X_c(\Delta H_m - T\Delta S_m)}{\alpha_N - 1} = \frac{X_c(T_m - T)\Delta S_m}{\alpha_N - 1} \tag{13}$$

which is just the same as that obtained by Iida.[14] In this equation T_m is the melting point of the crystal.

The necking stress extrapolated to 10^{-2} mm/min is drawn in Figure 11 as a function of temperature. The values by Iida[14] who measured σ_c as the relaxed stress at several seconds after draw was stopped, are also plotted in Figure 11. At high temperatures, the curve is almost linear and can be extrapolated to the melting point of polyethylene (141°C) at $\sigma_N = 0$. The slope $-d\sigma_N/dT$ gives $\Delta S/\Delta\alpha$ from eq. (12) and $X_c\Delta S_m/(\alpha_N - 1)$ from eq. (13). The observed value of $-d\sigma_N/dT$ is 0.63×10^6 dynes/(cm² deg). The calculated value from eq. (13), 0.67×10^6 dynes/(cm² deg), is in a satisfactory agreement with the observed value, as has been already

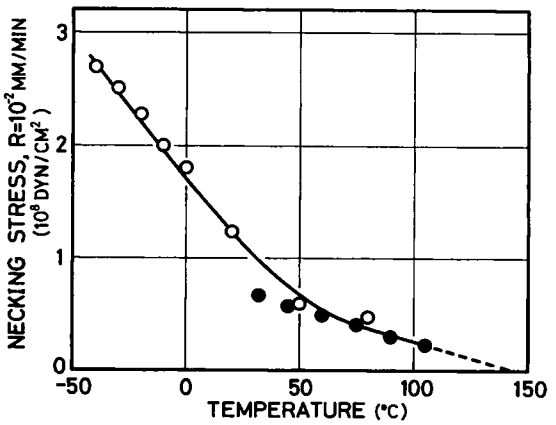

Fig. 11. Necking stress of high-density polyethylene at $R = 10^{-2}$ mm/min plotted against temperature. Closed circles represent data by Iida,[14] obtained as a relaxed stress at several seconds after draw has been stopped.

pointed out by Iida.[14] Values used in the calculation are $X_c = 0.9$ (degree of crystallinity of high-density polyethylene), $\Delta S_m = 68.5 \times 10^5$ erg/(deg cm^3) (entropy of fusion per unit volume), and α_N (observed value in Fig. 12). The agreement is rather astonishing, considering the crude approximations in eq. (13). The state B_2 is not liquid, as proved from x-ray study[9] and the density value. Actually, $X_c\Delta S_m > \Delta S$ and $(\alpha_N - 1) > \Delta\alpha$; but $X_c\Delta S_m/(\alpha_N - 1)$ might be nearly equal to $\Delta S/\Delta\alpha$; and consequently eq. (13) might be a good approximation of eq. (12).

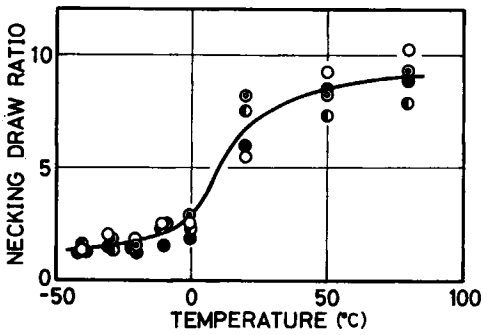

Fig. 12. Necking draw ratio of high-density polyethylene plotted against temperature for various draw rates: (O) 25; (⊙) 2.5; (◐) 0.25; (●) 0.025 mm/min.

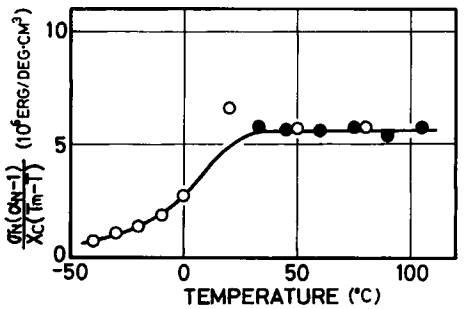

Fig. 13. Entropy of fusion, $\Delta S_m = \sigma_N(\alpha_N - 1)/X_c(T_M - T)$ plotted against temperature. Closed circles represent data taken from Iida.[14]

At low temperatures, however, σ_N at $R = 10^{-2}$ mm/min is higher than expected from linear extrapolation of high temperature values. This may result from the following: (1) σ_N at this draw rate is appreciably higher than σ_c at low temperatures where the relaxation time τ is long; (2) $\Delta\alpha$ becomes small at low temperatures, as illustrated in Figure 12.

Figure 13 gives $\sigma_N(\alpha_N - 1)/X_c(T_m - T)$, which might be equal to ΔS_m if $\sigma_N = \sigma_c$ and eq. (13) holds. The value decreases with decreasing temperature in a similar way to α_N in Figure 12. This is reasonable, because a small value of α_N indicates that the state B_2 is not well oriented, and consequently the entropy increase ΔS from B_1 to B_2 will be low.

Criterion of Cold Draw with Necking

In order to give a reason why necking does occur and uniform draw does not occur in high-density polyethylene, we must prove that the force required for draw is smaller in necking draw than uniform draw. In the following, we will describe the phenomenologic criterion of necking.

The volume element in the specimen is assumed to have a free energy density u (per unit volume), which is a function of the local draw ratio α,

$$u = u(\alpha) \tag{14}$$

where α takes the value from unity to α_0. When α reaches α_0, the volume element is transformed automatically to state C, accompanied with heat evolution, and the process of increase of α from unity to α_0 can be treated as an equilibrium problem. The density of the element is assumed to be independent of α.

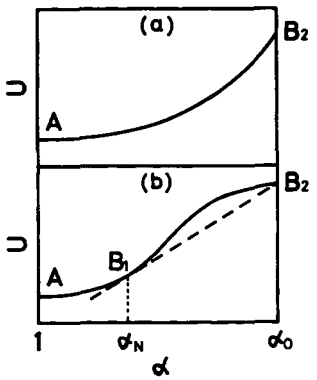

Fig. 14. Two typical cases of free energy density u plotted against local draw ratio α.

First, we calculate the force for uniform draw without necking. The energy of the whole specimen U and the length L are written in this case as

$$U = u(\alpha)LS = u(\alpha)L_iS_i, \; L = \alpha L_i \tag{15}$$

where S is the cross-sectional area and suffix i denotes the initial value. From eq. (15), the tensile force required for uniform draw is

$$F = \frac{dU}{dL} = S_i \frac{du}{d\alpha}. \tag{16}$$

Next, we consider draw with necking. If the fraction X of the specimen is in state $\alpha = \alpha_0$ and $(1 - X)$ in state $\alpha = \alpha_1$, $(\alpha_0 > \alpha_1)$, the total energy U' and the total length L' are

$$U' = L_iS_i(1 - X)u(\alpha_1) + L_iS_iXu(\alpha_0), \tag{17}$$

$$L' = L_i\alpha_1(1 - X) + L_i\alpha_0X.$$

Then the force for necking draw is

$$F' = \frac{dU'}{dL'} = \frac{dU'}{dX}\frac{dX}{dL'} = S_t \frac{u(\alpha_0) - u(\alpha_1)}{\alpha_0 - \alpha_1}. \tag{18}$$

This equation is the same as eq. (12).

Eqs. (16) and (18) indicate that conventional stress has a physical importance greater than that of true stress.

Since $\alpha = 1$ corresponds to the equilibrium state, $u(\alpha)$ is expanded in the vicinity of $\alpha = 1$ to

$$u(\alpha) = u(1) + {}^1/_2G(\alpha - 1)^2 + \ldots. \tag{19}$$

The curve $u(\alpha)$ versus α must therefore be concave upward from $\alpha = 1$ at least.

Two possible cases for $u(\alpha)$ are drawn in Figure 14. As is readily seen from eqs. (16) and (18), F/S_t as a function of α is given by the slope of the tangential line of $u(\alpha)$ and F'/S_t by the slope of the straight line connecting the point $u(\alpha_1)$ with the point $u(\alpha_0)$. In (a) of Figure 14, F is always smaller than F', and necking cannot be expected. In (b), the tangential line can be drawn from the point $u(\alpha_0)$ to curve $u(\alpha)$. The point of contact will be designated B_1 with $\alpha = \alpha_N$. Then, $F < F'$ for $\alpha < (1 + s_N)$, but $F > F'$ for $\alpha > \alpha_N$. The state B_1 is just the point where necking starts, or the yield point.

Some comments will be given here concerning stress peak at yielding. The stress peak is observed for high-density polyethylene under usual conditions, except at low temperatures and high draw rates, that is, at large values of $R\tau$. In these conditions, the stress–strain relation exhibits no peak but only a shoulder at which neck draw starts.

In order to discuss the yield stress, we must consider the energy barrier for motion of defects in state B_1. According to the scheme in Figure 10, the condition $u_1 = u_2$ is not sufficient to initiate necking, but a somewhat larger value of σ, the yielding stress σ_Y, is required for defects to move. Once the necking starts, the barrier is reduced by motion of defects, and the necking steadily continues at $\sigma = \sigma_N$. At low temperatures and high draw rates, however, σ_N, which is determined by the viscoelasticity of the amorphous phase, is higher than the stress to move defects, and the stress peak is not observed.

Discussions in this paper are based on the experimental results for high-density polyethylene. The model used is, however, quite general and may presumably apply to other crystalline polymers.

In conclusion, authors wish to express thanks to Dr. R. Hayakawa for valuable discussion.

References

1. S. W. Allison and R. D. Andrews, *J. Appl. Phys.*, **38**, 4164 (1967).
2. R. E. Robertson, *J. Appl. Polym. Sci.*, **7**, 443 (1963).
3. Yu S. Lazurkin and R. L. Fogel'son, *Zhur. Tekh. Fiz.*, **21**, 267 (1951).
4. I. Marshall and A. B. Thompson, *Proc. Roy. Soc., Ser. A*, **221**, 541 (1954).
5. P. I. Vincent, *Polymer*, **1**, 7 (1960).
6. J. C. Bauwens, C. Bauwens-Crowet, and G. Homes, *J. Polym. Sci.*, **7**, 1745 (1969).
7. S. W. Allison and I. M. Ward, *Brit. J. Appl. Phys.*, **18**, 1151 (1967).
8. S. J. Newman, *J. Appl. Polym. Sci.*, **2**, 252 (1959).
9. N. Kasai and M. Kakudo, *J. Polym. Sci.*, **A2**, 1955 (1964).
10. F. H. Müller, *Kolloid-Z. Z. Polym.*, **115**, 118 (1949); *ibid.*, **126**, 65 (1952).
11. F. H. Müller and K. Jäckel, *Kolloid-Z. Z. Polym.*, **129**, 145 (1952).
12. K. Jäckel, *Kolloid-Z. Z. Polym.*, **137**, 130 (1954).
13. A. Engelter and F. H. Müller, *Kolloid-Z. Z. Polym.*, **157**, 89 (1958).
14. S. Iida, Paper presented at the 18th Polymer Symposium, Tokyo, Japan, Nov. 1969.
15. A. Peterlin, *J. Polym. Sci.*, **C15**, 417 (1966).
16. Y. Wada, *J. Phys. Soc. Japan*, **16**, 1226 (1960).
17. O. Nakada, T. Hirai, and Y. Maeda, *Zairyo-Shiken*, **8**, 284 (1959).
18. J. D. Ferry, *Viscoelastic Properties of Polymers*, Wiley, New York, 1961, p. 201.
19. M. L. Williams, R. F. Landel, and J. D. Ferry, *J. Amer. Chem. Soc.*, **77**, 3701 (1955).

Received June 25, 1970
Revised October 8, 1970